MOLECULAR
IMAGING
AND BIOLOGY

World Molecular Imaging Society

imaging life
esmi
European Society for Molecular Imaging

CrossMark

## RESEARCH ARTICLE

# Association of Tumor [18F]FDG Activity and Diffusion Restriction with Clinical Outcomes of Rhabdomyosarcomas

Arian Pourmehdi Lahiji,[1] Tatianie Jackson,[1,2] Hossein Nejadnik,[1] Rie von Eyben,[3] Daniel Rubin,[1,4] Sheri L. Spunt,[5] Andrew Quon,[6] Heike Daldrup-Link[1,5]

[1]The Department of Radiology and Molecular Imaging Program at Stanford (MIPS), Stanford University School of Medicine, 725 Welch Rd, Rm 1665, Stanford, CA, 94305-5654, USA

[2]Department of Radiology, Boston University Medical Center, Boston, MA, USA

[3]Department of Radiation Oncology, Stanford University School of Medicine, Stanford, CA, USA

[4]Department of Biomedical Data Science, Stanford University School of Medicine, Stanford, CA, USA

[5]Department of Pediatrics, Division of Hematology/Oncology, Stanford University School of Medicine, Stanford, CA, USA

[6]Department of Nuclear Medicine, Stanford University School of Medicine, Stanford, CA, USA

### Abstract

*Purpose:* To evaluate whether the extent of restricted diffusion and 2-deoxy-2-[18F] fluoro-D-glucose ([18F]FDG) uptake of pediatric rhabdomyosarcomas (RMS) on positron emission tomography (PET)/magnetic resonance (MR) images provides prognostic information.

*Procedure:* In a retrospective, IRB-approved study, we evaluated [18F]FDG PET/CT and diffusion-weighted (DW) MR imaging studies of 21 children and adolescents (age 1–20 years) with RMS of the head and neck. [18F]FDG PET and DW MR scans at the time of the initial tumor diagnosis were fused using MIM software. Quantitative measures of the tumor mass with restricted diffusion, [18F]FDG hypermetabolism, or both were dichotomized at the median and tested for significance using Gray's test. Data were analyzed using a survival analysis and competing risk model with death as the competing risk.

*Results:* [18F]FDG PET/MR images demonstrated a mismatch between tumor areas with increased [18F]FDG uptake and restricted diffusion. The DWI, PET, and DWI + PET tumor volumes were dichotomized at their median values, 23.7, 16.4, and 9.5 cm$^3$, respectively, and were used to estimate survival. DWI, PET, and DWI + PET overlap tumor volumes above the cutoff values were associated with tumor recurrence, regardless of post therapy COG stage ($p = 0.007$, $p = 0.04$, and $p = 0.07$, respectively).

*Conclusion:* The extent of restricted diffusion within RMS and overlap of hypermetabolism plus restricted diffusion predict unfavorable clinical outcomes.

**Key words:** Rhabdomyosarcoma, [18F]FDG, Diffusion-weighted MR, PET/MR

Arian Pourmehdi Lahiji and Tatianie Jackson are both co-first authors

*Correspondence to:* Heike Daldrup-Link; *e-mail:* H.E.Daldrup-Link@stanford.edu

## Introduction

Soft tissue sarcomas represent the most common extra-cranial solid malignancies in children and adolescents with an age of less than 20 years [1, 2]. The majority of soft tissue sarcomas in children are rhabdomyosarcoma (RMS), with embryonal and

alveolar histological subtypes accounting for approximately 350 new pediatric tumors per year [1]. Since 1972, the Intergroup Rhabdomyosarcoma Study Group, which has since become the Soft Tissue Sarcoma Committee of the Children's Oncology Group (COG), has conducted clinical trials aimed at improving the outcome for pediatric patients with RMS [1]. While the overall survival of patients with localized disease has significantly improved as a result of these efforts, the overall survival for patients with advanced disease continues to be less than 30 %. Clinical routine cross-sectional imaging is poor at predicting clinical outcomes [3, 4]. More detailed information is required at baseline in order to stratify high-risk patients to personalized therapies.

Prognostic biomarkers aim to differentiate less aggressive tumors with a high likelihood of cure, which could be treated less aggressively, and more aggressive tumors with low likelihood of cure, which require aggressive therapeutic plans. Established prognostic biomarkers for patients with RMS are age, tumor size, location, grade/histology, stage, and surgical resectability at initial presentation [1]. Morphological characteristics of RMS on conventional cross-sectional CT and MR imaging studies are relatively non-specific [5]. The presence and distribution of metastases at the time of diagnosis has been established as an important prognostic factor [6]. However, few studies have investigated the prognostic value of advanced imaging tools, such as diffusion-weighted imaging (DWI) and 2-deoxy-2-[$^{18}$F] fluoro-D-glucose ([$^{18}$F]FDG) positron emission tomography (PET), which provide information about biological tumor characteristics such as tumor cell density (DWI) and metabolic activity ([$^{18}$F]FDG-PET). Previous studies reported that the degree of metabolic activity of the primary tumor at the time of initial diagnosis, as measured on [$^{18}$F]FDG PET scans, can predict survival in pediatric sarcoma patients [7–9]. In addition, it has been reported that the degree of restricted diffusion on DWI can provide prognostic information [10, 11]. However, no universally applicable thresholds of restricted diffusion or metabolic activity have been defined that can reliably predict outcomes. This may be due to high variability in techniques and equipment [12]. Since pediatric RMS are typically very heterogeneous, we hypothesized that the extent, rather than the degree, of restricted diffusion and [$^{18}$F]FDG hypermetabolism in the tumor tissue may be more robust measures of tumor aggressiveness. Therefore, the purpose of our study was to evaluate whether the extent of restricted diffusion (surrogate for high cell density) and [$^{18}$F]FDG uptake (tumor metabolism) on fused PET/MR images before start of chemotherapy provides prognostic information about clinical outcomes.

# Materials and Methods

## Study Patients

The Institutional Review Board at our institution approved this retrospective study. Twenty-one pediatric patients and young adults with rhabdomyosarcomas of the head and neck, including 7 girls and 14 boys with an age of 1–

20 years (mean $10.04 \pm 5.52$ SD), underwent a baseline [$^{18}$F]FDG PET and DWI-MR scan at the time of disease diagnosis, before start of chemotherapy. Six patients had an intermediate-risk alveolar rhabdomyosarcoma and 15 patients had an embryonal rhabdomyosarcoma. The children were all enrolled in the COG ARST0531 study and randomized to chemotherapeutic regimen consisting of vincristine, dactinomycin, and cyclophosphamide (VAC) or VAC alternating with vincristine and irinotecan (VI) over 43 weeks. The overall goal of the ARST0531 protocol was to increase the cure rate without causing more serious side effects from treatment. We focused our analyses on head and neck tumors, because these are often not primarily resected. This allowed us to correlate quantitative imaging data at baseline with RECIST criteria after induction chemotherapy.

## Imaging

The imaging workflow consisted of [$^{18}$F]FDG PET scans and MRI scans at baseline, 15, 30, and 43 weeks. Fifteen patients were imaged with General Electric (GE) Healthcare scanners, 4 patients with Siemens scanners, and 2 with Philips scanners. MRI scans consisted of axial and/or coronal fat-saturated T2-weighted fast spinecho scans as well as axial and/or coronal T1-weighted fast spinecho or gradient echo scans before and after intravenous injection of gadolinium chelates. Diffusion-weighted (DW) MR scans were acquired at the discretion of the treating institution with variable repetition times, variable echo times, and variable b-values, ranging from $b = 600$ to $b = 1000$ ms. In preparation for a positron emission tomography (PET) scan, patients were asked to limit carbohydrate intake for 24 h before the scan and to not eat anything (except drinking water) for 6 h before the scan. Before injection of [$^{18}$F]FDG, a blood glucose test was obtained to confirm a blood glucose concentration of less than 150 mg/dl. At approximately 60 min after intravenous injection of [$^{18}$F]FDG at a dose of 3–5 MBq/kg, low-dose CT images and PET images were obtained. PET data were attenuation corrected by CT data and reconstructed in axial, sagittal, and coronal planes. The sequentially obtained [$^{18}$F]FDG PET and MRI data were aligned and fused with MIM software using non-rigid fusion function.

MRI and PET scans were obtained sequentially, aligned and fused with MIM software using the non-rigid fusion function. Using skeletal muscle as an internal standard for normal background tissue, tumor areas with increased [$^{18}$F]FDG uptake, restricted diffusion or both (compared to background) were manually outlined on each image slice. The MIM software automatically calculated the tumor mass in the region of interest (ROI) with restricted diffusion, increased [$^{18}$F]FDG uptake, or both. The whole tumor was also measured on anatomical MR scans, and the relative tumor volume that showed increased [$^{18}$F]FDG avidity, restricted diffusion, or both was calculated as ROI tumor volume/whole tumor volume × 100 % (Figs. 2 and 3). In

addition, tumor SUVmax were determined with MIM software and ADC values were measured with Osirix software.

## Clinical Outcomes

Follow-up MRI scans at 15 weeks after initiation of chemotherapy were used to categorize tumors as complete responders, partial responders, stable disease, or progressive disease, according to COG staging and RECIST size criteria [1, 13]. Two of our patients achieved complete response, 16 patients partial response, 2 patients stable disease, and 1 patient progressive disease. Patients with partial or complete response were categorized as responders and patients with stable or progressive disease were categorized as non-responders. In addition, we recorded post-therapy follow-up data at 5 years after completion of therapy, provided by the COG-STS ARST0531 study team. COG classified event-free survival as the absence of local or metastatic recurrence/progression. Out of 21 patients, 11 patients were event free at 5 years, and 10 patients developed disease progression before 5 years.

## Statistical Analyses

Quantitative measures of tumor volumes, SUVmax, or ADC values were compared between alveolar and embryonal RMS as well as responders and non-responders using $t$ tests. In addition, SUVmax, ADC values, and quantitative measures of the absolute or relative tumor mass with restricted diffusion, [18F]FDG hypermetabolism, or both were dichotomized at the median and then tested for significance using Gray's test. Data were analyzed using a survival analysis and competing risk model with death as the competing risk. Significant differences were assigned for a $p$ value of less than 0.05.

# Results

Fused [18F]FDG PET/MR images at baseline demonstrated marked heterogeneity of all RMS with mismatch of tumor areas that showed increased [18F]FDG uptake and restricted diffusion. There was no significant difference between alveolar and embryonal RMS with regard to the extent or degree of restricted diffusion, [18F]FDG hypermetabolism, or both ($p > 0.05$).

The relative tumor proportion at baseline (percent tumor area) with both restricted diffusion and FDG hypermetabolism was inversely related to tumor response (Fig. 1): Tumors with low overlap of restricted diffusion and [18F]FDG hypermetabolism at baseline showed subsequent response to chemotherapy (Fig. 2), while tumors with high overlap of restricted diffusion and [18F]FDG hypermetabolism at baseline showed stable or progressive disease on follow-up scans (Fig. 3).

The same tumors did not show a significant difference in tumor size at baseline: Responders according to RECIST criteria demonstrated an average tumor diameter of 3.8 cm at baseline (range 2.6–5.0 cm) and 1.6 cm after 15 months of therapy (range 0.78–2.6 cm). Non-responders according to RECIST criteria demonstrated an average tumor diameter of 3.8 cm at baseline (range 3.2–4.4 cm) and 4.4 cm after 15 months of therapy (range 2.7–6.0 cm).

Next, the DWI MRI, [18F]FDG PET, and DWI MRI+[18F]FDG PET tumor volumes were dichotomized at their median values, 23.7, 16.4, and 9.5 cm$^3$, respectively, and used as prospective criteria to predict event-free survival. DWI, PET, and DWI + PET overlap tumor volumes above the cut-off values were associated with tumor progression, regardless of post-therapy COG stage ($p = 0.007$, $p = 0.04$, and $p = 0.07$, respectively). Patients with a DWI volume greater than 23.7 cm$^3$ had a significantly higher cumulative incidence of tumor progression than patients with a DWI volume less than 23.7 cm$^3$ ($p = 0.007$). The patients with higher DWI + PET overlap or PET volume had a higher cumulative incidence of progression that approached statistical significance ($p = 0.07$ and $p = 0.04$) (Fig. 4). However, the relative tumor volume with DWI, PET, and PET + DWI did not show any significant difference in cumulative incidence of progression of tumors ($p > 0.05$).

In addition to the extent of restricted diffusion and [18F]FDG hypermetabolism within the tumor tissue, we also evaluated the degree of restricted diffusion and [18F]FDG hypermetabolism: Responders had a mean tumor SUVmax of $7.1 \pm 3.69$ and a mean ADC value of $1041.7 \pm 448.7$. Non-responders had a mean tumor SUVmax of $5.1 \pm 3.09$ and a mean ADC value of $799.2 \pm 623.1$. These differences were not significantly different between responders and non-responders ($p = 0.17$ and $p = 0.30$, respectively). The ADC and SUVmax values were also dichotomized based on their median values and were not significantly related to cumulative incidence of progression ($p = 0.24$ and $p = 0.52$) (Fig. 5).

# Discussion

Our data showed that the extent of restricted diffusion in pediatric RMS at baseline and the extent of combined restricted diffusion plus [18F]FDG hypermetabolism can be used as prognostic biomarkers for event-free survival in pediatric RMS, independent of RECIST-based response assessments, ADC values, and SUV values.

Therapy stratifications for RMS are currently based on demographical and anatomical criteria, such as patient age and disease bulk, location, and distribution (local vs. systemic tumor spread). In 2000, the COG-STS and Intergroup Rhabdomyosarcoma Study Group IRSG [1, 14] defined low-, intermediate-, and high-risk groups, based on histology, stage, and surgical pathology [1]. However, improvement of overall survival (OS) has been slow.
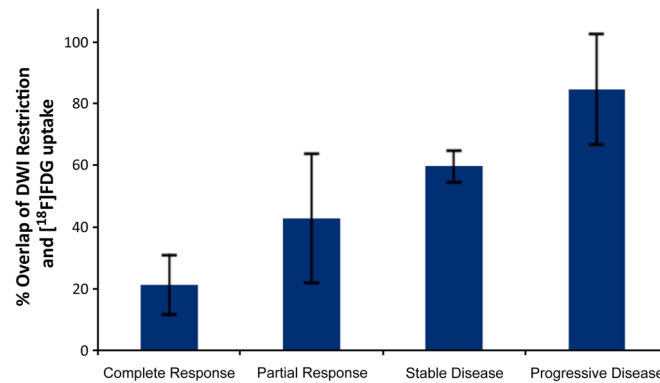
**Fig. 1.** Predictive value of the relative tumor volume with combined restricted diffusion and [18F]FDG hypermetabolism in RMS. Mean tumor volume with both restricted diffusion and [18F]FDG hypermetabolism at baseline (calculated as DWI and [18F]FDG positive tumor volume/whole tumor volume × 100 %) increases with decreasing response to chemotherapy, as determined by RECIST criteria at 15 weeks after start of chemotherapy ($p < 0.0001$). Data are displayed as mean values for each response group and standard deviations.

Ognjanovic et al. observed no improvement in the 5-year survival rate of pediatric ARMS based on the SEER database, while children with ERMS had no change in their 5-year survival rate [2]. Classical imaging criteria to determine treatment effects are based on tumor size measurements AFTER chemotherapy according to RECIST (response evaluation criteria in solid tumors) [15] and PERCIST criteria (positron emission tomography response criteria in solid tumors) [15]. A significant decline in tumor size and decline in FDG metabolism after chemotherapy has been linked to favorable overall survival of patients with malignant lymphomas and sarcomas [16–18]. However, in Ewing sarcomas, this criterion has been less useful as both responders and non-responders showed a decline in tumor [18F]FDG uptake after induction therapy. It was suggested that in these tumors, an earlier follow-up scan might be a
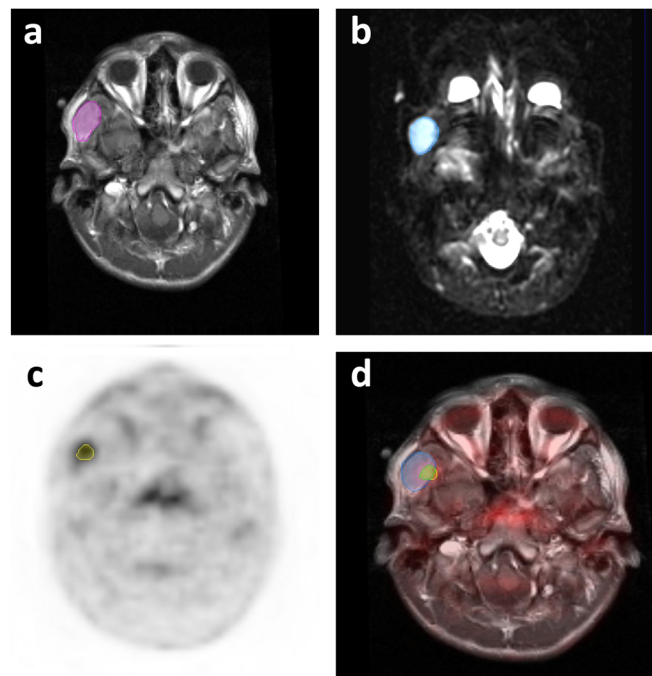


**Fig. 2.** [18F]FDG PET and MR scans of a 16-year-old boy with right temporal alveolar rhabdomyosarcoma. **a** Manually drawn ROI outlines the whole tumor on contrast-enhanced T1-weighted image. **b** ROI outlines tumor mass with restricted diffusion on diffusion weighted MRI scan. **c** ROI outlines tumor mass with increased [18F]FDG metabolic activity on PET. **d** Fourteen percent of the whole tumor tissue showed overlap of [18F]FDG metabolic activity and restricted diffusion. The child achieved complete response after therapy and has an event-free survival of more than 5 years.
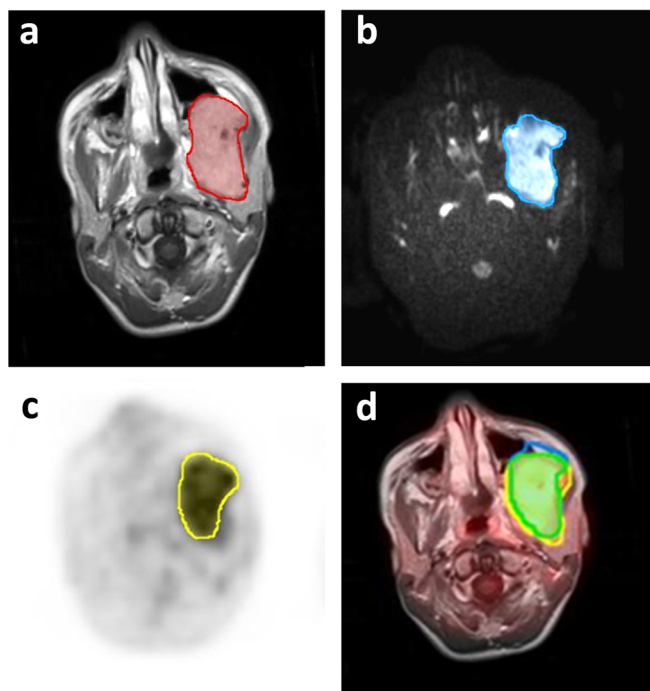
**Fig. 3.** [18F]FDG PET and MR scans of a 6-year-old girl with left nasopharyngeal embryonal rhabdomyosarcoma before start of therapy. **a** Manually drawn region of interest (ROI) outlines the whole tumor mass on contrast-enhanced T1 weighted image. **b** ROI outlines tumor mass with restricted diffusion. **c** ROI outlines tumor mass with increased [18F]FDG metabolic activity on PET. **d** Eighty-eight percent of the tumor tissue showed an overlap of [18F]FDG metabolic activity and restricted diffusion. The patient demonstrated progressive disease at 2.4 years after therapy.

better indicator of differential response of these two groups [19]. Currently, most COG (Children's Oncology Group) protocols are based on tumor SUV values that are calculated based on the patient's body weight. In children, calculating SUV values based on the patient's body surface area might lead to better results [20].

Our data suggest a new, independent, and robust prognostic imaging biomarker: The extent of restricted diffusion (as a measure of tumor cell density). This is in accordance with studies by Cuccarini et al., who reported that normalized ADC values and restricted diffusion (increased tumor cellularity) were directly associated with anaplastic progression of high-grade gliomas [21].

It is notable that we found a non-significant correlation between the extent of FDG activity and clinical outcomes. While tumors in this study did not contain obvious necrosis on contrast-enhanced MRI scans, some showed a central photopenic area on [18F]FDG PET scans. The same tumors showed peripheral and centrally restricted diffusion. This mismatch deserves further studies.

We did not find a significant relation between SUVmax at baseline and response to chemotherapy at week 15 or event-free survival after 5 years. Two reasons can explain this observation: (i) SUVmax in different histologic types of STS increase with tumor grade, but not with the size of the lesion [22]. (ii) Activation of phosphatidylinositol 3-kinase/serine/threoneine kinase in the proper cell type and microenvironment can activate hypoxia-inducible factor-1 in RMS

cells, which has been proven to impede the glycolytic rate of [18F]FDG [23].

Several previous studies found positive correlations between the metabolic activity of a primary tumor, as diagnosed on a PET scan, and clinical outcomes: In pediatric patients with rhabdomyosarcomas, Baum and coworkers reported an inverse relation between primary tumor SUV max and survival [7]. In patients with Ewing sarcomas, Gupta and co-workers found a significantly higher SUV max for metastasized compared to non-metastasized tumors [24]. In patients with Wilms tumors, Begent and coworkers found significantly higher SUVmax of high-risk tumors compared to low-risk tumors [25]. Other investigators also reported that [18F]FDG PET/CT can predict survival in pediatric sarcoma patients [7–9]. In a study on 41 RMS patients, detection of hypermetabolism in the primary tumor with an SUVmax/SUVliver of more than 4.6 was an indicator of lower survival rates [7]. In the same cohort, only 56 % of patients with high-intensity primary tumors that had [18F]FDG uptake close to brain activity at initial diagnosis survived for more than 49 months, whereas all patients with low-intensity primary tumors that had [18F]FDG uptake lower than or equal to liver activity survived [7]. Unfortunately, we did not find similar results. One reason can be the scan variability of a multicenter cohort, with images acquired with different imaging procedures, technologies, and scanners. Previous
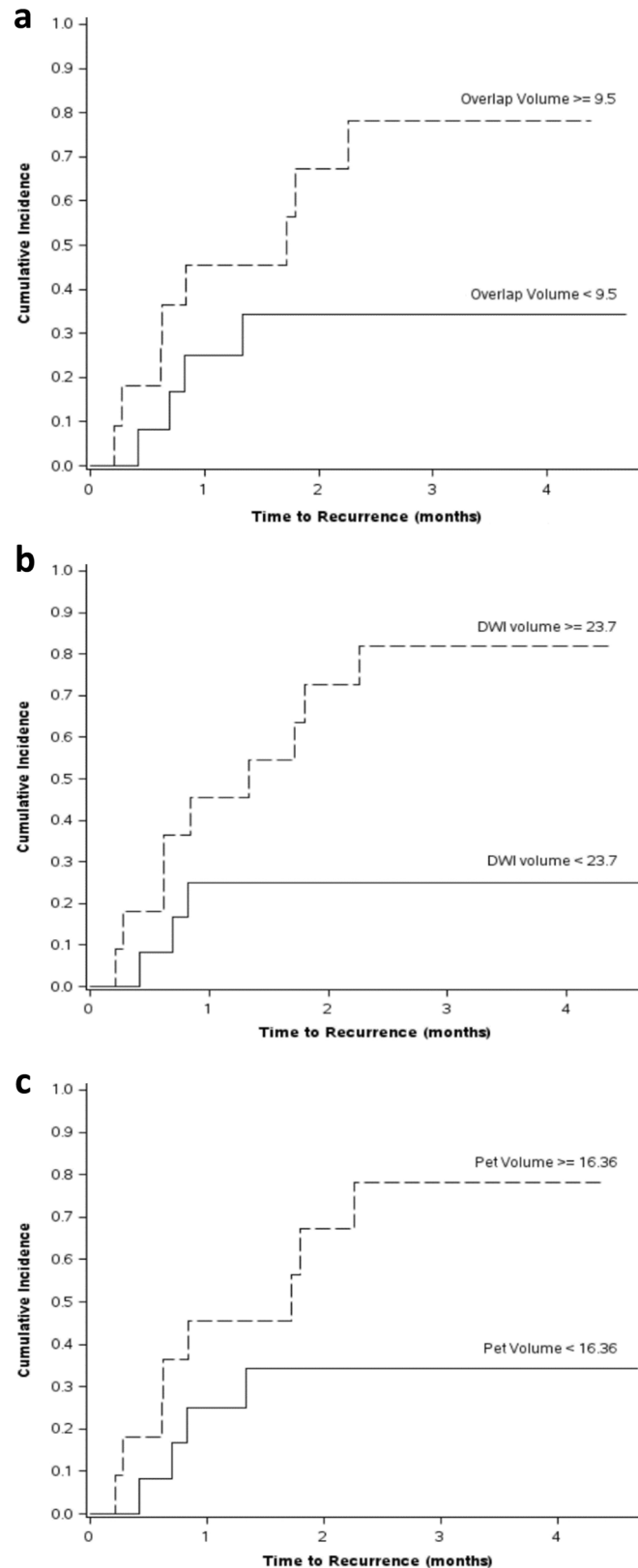
Fig. 4. **a** Competing risk model of [$^{18}$F]FDG PET and DWI overlap volume dichotomized according to a median cut-off of 9.5 cm$^3$. Children with a tumor mass with combined [$^{18}$F]FDG uptake and restricted diffusion of greater than 9.5 cm$^3$ had an increased risk for recurrence within 5 years ($p = 0.07$). **b** Competing risk model of DWI volume dichotomized according to a median cut-off of $>23.7$cm$^3$. Children with DWI volume $>23.7$ cm$^3$ had an increased risk for recurrence within 5 years ($p = 0.007$). **c** Competing risk model of [$^{18}$F]FDG avid tumor volume dichotomized according to a median cut-off of 16.4 cm$^3$. Children with [$^{18}$F]FDG avid tumor volume $> 16.4$ cm$^3$ had an increased risk for recurrence within 5 years ($p = 0.04$).
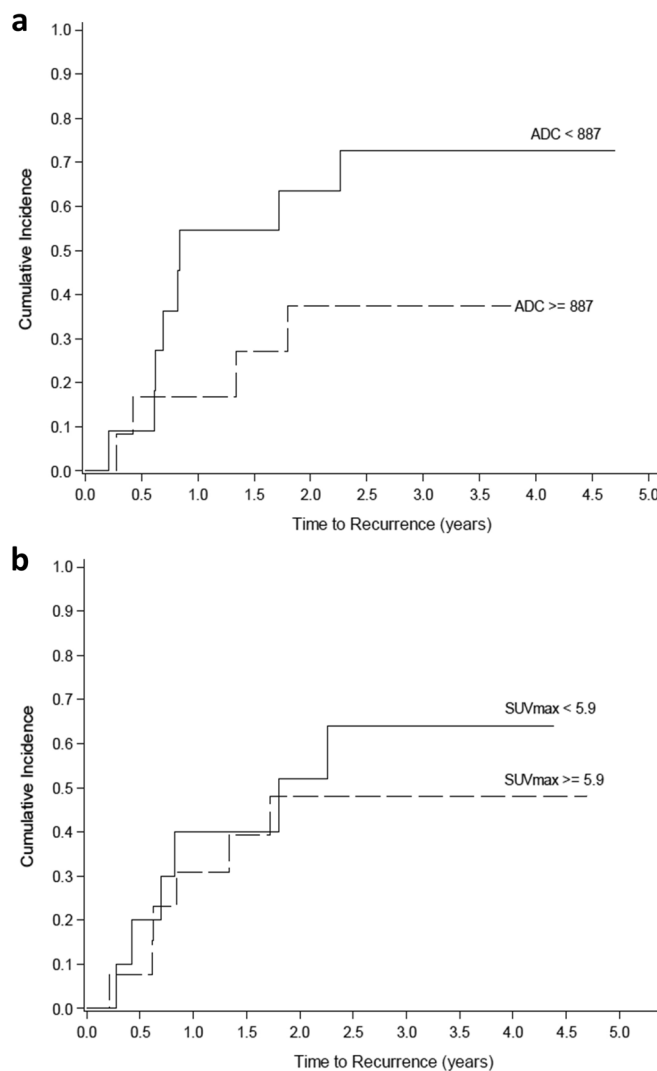
Fig. 5. **a** ADC and **b** SUVmax values were dichotomized based on their median values and were not significantly related to cumulative incidence of progression ($p = 0.244$ and $0.521$).

investigators have shown variable SUVs with different imaging algorithms: Oldan et al. demonstrated improvement in contrast recovery with "time of flight (TOF)" PET/CT *versus* non-TOF PET/CT reconstruction, which clinically has higher SUV uptake structures [12]. Furthermore, most multicenter trials reported difficulty standardizing [$^{18}$F]FDG-radiotracer uptake time. Kurland et al. reported that uptake time variations from 45 to 120 min have a marked impact on measured SUV and decrease reliability of [$^{18}$F]FDG PET response biomarkers [26]. Our data show that the extent rather than degree of tumor-restricted diffusion may be a more robust predictive and prognostic biomarker.

We recognize several limitations of our study: Although our patient cohort seems to be the largest cohort of pediatric rhabdomyosarcomas examined with MRI and PET to date, the patient numbers in responder and non-responder groups are relatively small. MR and [$^{18}$F]FDG PET imaging scans collected through a multicenter dataset were obtained with a variety of approaches and technical equipment, which represents current clinical practice. These data were secondarily fused, using well-established fusion strategies [27, 28]: Therefore, unavailability of an integrated PET/MR system does not limit the use of combined FDG and DWI information in clinical practice.

## Conclusion

Our study shows that DWI tumor volume is a statically significant prognostic biomarker for clinical outcomes of pediatric RMS. These results might motivate future studies to include DW information into ongoing clinical trials.

**Compliance with Ethical Standards**

*Conflict of Interest*

The authors declare that they have no conflict of interest.

*Ethical Approval*

All procedures performed in studies involving human participants were in accordance with the Institutional Review Board at our institution and with the 1964 Helsinki declaration and its later amendments or comparable ethical standards."

## References

1. Malempati S, Hawkins DS (2012) Rhabdomyosarcoma: review of the Children's Oncology Group (COG) soft-tissue sarcoma committee experience and rationale for current COG studies. Pediatr Blood Cancer 59:5–10
2. Ognjanovic S, Linabery AM, Charbonneau B, Ross JA (2009) Trends in childhood rhabdomyosarcoma incidence and survival in the United States, 1975-2005. Cancer 115:4218–4226
3. Rodeberg DA, Stoner JA, Hayes-Jordan A, Kao SC, Wolden SL, Qualman SJ, Meyer WH, Hawkins DS (2009) Prognostic significance of tumor response at the end of therapy in group III rhabdomyosarcoma: a report from the children's oncology group. J Clin Oncol 27:3705–3711
4. Kleis M, Daldrup-Link H, Matthay K, Goldsby R, Lu Y, Schuster T, Schreck C, Chu PW, Hawkins RA, Franc BL (2009) Diagnostic value of PET/CT for the staging and restaging of pediatric tumors. Eur J Nucl Med Mol Imaging 36:23–36
5. Voss SD (2011) Pediatric oncology and the future of oncological imaging. Pediatr Radiol 41(Suppl 1):S172–S185
6. Lager JJ, Lyden ER, Anderson JR et al (2006) Pooled analysis of phase II window studies in children with contemporary high-risk metastatic rhabdomyosarcoma: a report from the soft tissue sarcoma committee of the children's oncology group. J Clin Oncol 24:3415–3422
7. Baum SH, Fruhwald M, Rahbar K, Wessling J, Schober O, Weckesser M (2011) Contribution of PET/CT to prediction of outcome in children and young adults with rhabdomyosarcoma. J Nucl Med 52:1535–1540
8. Franzius C, Bielack S, Flege S, Sciuk J, Jürgens H, Schober O (2002) Prognostic significance of $^{18}$F-FDG and $^{99m}$Tc-methylene diphosphonate uptake in primary osteosarcoma. J Nucl Med 43:1012–1017
9. Brenner W, Conrad EU, Eary JF (2004) FDG PET imaging for grading and prediction of outcome in chondrosarcoma patients. Eur J Nucl Med Mol Imaging 31:189–195
10. Padhani AR, Liu G, Mu-Koh D, Chenevert TL, Thoeny HC, Takahara T, Dzik-Jurasz A, Ross BD, van Cauteren M, Collins D, Hammoud DA, Rustin GJS, Taouli B, Choyke PL (2009) Diffusion-weighted magnetic resonance imaging as a cancer biomarker: consensus and recommendations. Neoplasia 11:102–125
11. Afaq A, Andreou A, Koh D (2010) Diffusion-weighted magnetic resonance imaging for tumour response assessment: why, when and how? Cancer Imaging 10:S179–S188
12. Oldan JD, Turkington TG, Choudhury K, Chin BB (2015) Quantitative differences in [(18)F] NaF PET/CT: TOF versus non-TOF measurements. Am J Nucl Med Mol Imaging 5:504–514
13. Ferrari A, Miceli R, Meazza C, Casanova M, Favini F, Morosi C, Trecate G, Marchianò A, Luksch R, Cefalo G, Terenziani M, Spreafico F, Polastri D, Podda M, Catania S, Schiavello E, Giannatempo P, Gandola L, Massimino M, Mariani L (2010) Comparison of the prognostic value of assessing tumor diameter versus tumor volume at diagnosis or in response to initial chemotherapy in rhabdomyosarcoma. J Clin Oncol 28:1322–1328
14. Ries LAG SM, Gurney JG, Linet M, et al. (2005) Cancer incidence and survival among children and adolescents. National Cancer Institute, SEER Program
15. Wahl RL, Jacene H, Kasamon Y, Lodge MA (2009) From RECIST to PERCIST: evolving considerations for PET response criteria in solid tumors. J Nucl Med 50(Suppl 1):122s–150s
16. Bakhshi S, Radhakrishnan V, Sharma P, Kumar R, Thulkar S, Vishnubhatla S, Dhawan D, Malhotra A (2012) Pediatric nonlymphoblastic non-Hodgkin lymphoma: baseline, interim, and posttreatment-enhanced CT for evaluation—a prospective study. Radiology 262:956–968
17. Riad R, Omar W, Kotb M, Hafez M, Sidhom I, Zamzam M, Zaky I, Abdel-Dayem H (2010) Role of PET/CT in malignant pediatric lymphoma. Eur J Nucl Med Mol Imaging 37:319–329
18. Bestic JM, Peterson JJ, Bancroft LW (2009) Pediatric FDG PET/CT: physiologic uptake, normal variants, and benign conditions [corrected]. Radiographics 29:1487–1500
19. Uslu L, Donig J, Link M, Rosenberg J, Quon A, Daldrup-Link HE (2015) Value of $^{18}$F-FDG PET and PET/CT for evaluation of pediatric malignancies. J Nucl Med 56:274–286
20. Kim CK, Gupta NC, Chandramouli B, Alavi A (1994) Standardized uptake values of FDG: body surface area correction is preferable to body weight correction. J Nucl Med 35:164–167
21. Cuccarini V, Erbetta A, Farinotti M et al (2015) Advanced MRI may complement histological diagnosis of lower grade gliomas and help in predicting survival. J Neuro-Oncol 126:279–288
22. Schwarzbach MH, Dimitrakopoulou-Strauss A, Willeke F et al (2000) Clinical value of [$^{18}$F] fluorodeoxyglucose positron emission tomography imaging in soft tissue sarcomas. Ann Surg 231:380–386
23. Kilic-Eren M, Boylu T, Tabor V (2013) Targeting PI3K/Akt represses hypoxia inducible factor-1α activation and sensitizes rhabdomyosarcoma and Ewing's sarcoma cells for apoptosis. Cancer Cell Int 13:36
24. Gupta K, Pawaskar A, Basu S, Rajan MGR, Asopa RV, Arora B, Nair N, Banavali S (2011) Potential role of FDG PET imaging in predicting metastatic potential and assessment of therapeutic response to neoadjuvant chemotherapy in Ewing sarcoma family of tumors. Clin Nucl Med 36:973–977
25. Begent J, Sebire NJ, Levitt G et al (2011) F(18)-Fluorodeoxyglucose Positron Emission Tomography/computerised tomography in Wilms' tumour: correlation with conventional imaging, pathology and immunohistochemistry. Eur J Cancer 47:389–396
26. Kurland BF, Muzi M, Peterson LM, Doot RK, Wangerin KA, Mankoff DA, Linden HM, Kinahan PE (2016) Multicenter clinical trials using $^{18}$F-FDG PET to measure early response to oncologic therapy: effects of injection-to-acquisition time variability on required sample size. J Nucl Med 57:226–230
27. Antonica F, Asabella AN, Ferrari C et al (2014) Useful diagnostic biometabolic data obtained by PET/CT and MR fusion imaging using open source software. Hellenic. J Nucl Med 17(Suppl 1):50–55
28. Zaidi H, Montandon ML, Alavi A (2010) The clinical role of fusion imaging using PET, CT, and MR imaging. Magn Reson Imaging Clin 18:133–149